ACS APPLIED MATERIALS & INTERFACES

Research Article

www.acsami.org

Facile Synthesis of Gold@Graphitized Mesoporous Silica Nanocomposite and Its Surface-Assisted Laser Desorption/Ionization for Time-of-Flight Mass Spectroscopy

Guiju Xu,[†,‡] Shengju Liu,[†,‡] Jiaxi Peng,[†,‡] Wenping Lv,[†] and Ren'an Wu*[,†]

[†]CAS Key Laboratory of Separation Science for Analytical Chemistry, National Chromatographic R&A Center, Dalian Institute of Chemical Physics, Chinese Academy of Sciences (CAS), Dalian 116023, China

[‡]University of Chinese Academy of Sciences, Beijing 100049, China

Supporting Information

ABSTRACT: In this work, a novel core–shell structured gold@graphitized mesoporous silica nanocomposite (Au@GMSN) was synthesized by in situ graphitization of template within the mesochannels of mesoporous silica shell on gold core and demonstrated to be promising nanomaterials for surface-assisted laser desorption/ionization time-of-flight mass spectroscopy (SALDI-TOF MS). The integration of the graphitized mesoporous silica with the gold nanoparticles endowed Au@GMSN with large surface areas of graphitic structure, good dispersibility, and strong ultraviolet (UV) absorption. Au@GMSN exerted the synergistic effect on the efficient detection of small-molecular-weight analytes including amino acids, neutral saccharides, peptides, and traditional Chinese medicine. The Au@GMSN-assisted laser desorption/ionization exhibited the following superiorities: high ionization efficiency, low fragmentation interference, favorable salt tolerance, and good reproducibility. Moreover, because of the large hydrophobic inner surface area of the graphitized mesoporous silica shell, the Au@GMSN demonstrated its promising capacity in the pre-enrichment of aromatic analytes prior to SALDI-TOF MS, which favored rapid and sensitive detection.

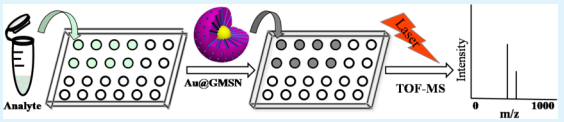

KEYWORDS: *gold, graphitized mesoporous silica, core–shell, SALDI-TOF MS*

INTRODUCTION

Matrix-assisted laser desorption/ionization time-of-flight mass spectrometry (MALDI-TOF MS) has become a powerful technique for biochemical analysis and proteomics research,[1−3] with the aid of ultraviolet (UV)-absorbable organic compounds (e.g., 2,5-dihydroxybenzoic acid (DHB), α-cyano-4-hydroxycinnamic acid (CHCA), or trans-3,5-dimethoxy-4-hydroxycinnamic acid (SA) etc.) as organic matrixes. Nevertheless, the presence of abundant interfering matrix peaks in the low-mass range makes MALDI-TOF MS incapable of detecting small molecules (m/z < 500 Da).[4] In addition, the inhomogeneous co-crystallization of analytes with an organic matrix requires sweet-spot searching, which thereby leads to poor region-to-region and sample-to-sample reproducibility.[5] To hurdle these problems, organic-matrix-free laser desorption/ionization mass spectrometry, that is, surface-assisted laser desorption/ionization time-of-flight mass spectrometry (SALDI-TOF MS), has been developed.[6] The SALDI-TOF MS technique utilizes nanostructured substrates (e.g., porous silicon,[7] silicon nanowire arrays,[8,9] self-assembled germanium nanodots,[10] and platinum nanoflowers on scratched silicon[11]) or nanomaterials (e.g., carbon nanotubes,[12−14] carbon nanodots,[15] graphene,[16−19] gold nanoparticles,[20,21] and mesoporous silica[22]) to transfer laser energy to the analytes for ionization, which could minimize the background interference of organic matrixes in low-mass range, avoid the complication of co-crystallization between analytes and matrix, and thereby provide improved reproducibility and sensitivity.

To achieve sensitive and reproducible SALDI-TOF MS, not only efficient laser energy absorption, but also the homogeneous dispersion of the surface-assisted nanomaterials on the plate, are critical.[23] Because of their strong absorption in the UV region, high conductivity, excellent thermal stability, and high energy transfer efficiency of graphitic structure, the carbon-based nanomaterials have emerged as a promising material for SALDI-TOF MS.[24−26] However, it should be noted that the pristine carbon-based nanomaterials display low solubility and poor dispersibility in solution, leading to their inhomogeneous distribution on sample wells and, thereby, the unsatisfied reproducibility during SALDI analysis, without the complicated modification.[14,27−29] Therefore, it is highly desirable to develop nanomaterials combined with the large surface areas of graphitic structure and inherent good dispersibility, which could improve the laser desorption/ionization (LDI) efficiency and prevent inhomogeneous distribution.

In this study, we demonstrate a facile method to synthesize a core–shell structured gold@graphitized mesoporous silica nanocomposite (Au@GMSN) by in situ graphitization of the

Received: November 11, 2014
Accepted: December 31, 2014
Published: December 31, 2014

DOI: 10.1021/am507894y
ACS Appl. Mater. Interfaces 2015, 7, 2032−2038

template within the mesochannels of mesoporous silica shell on gold core. The graphitized carbon deposited on the inner surface of the mesoporous silica shell yields a large graphitized hydrophobic inner surface area[30] and strong UV adsorption.[31] The outer hydrophilic mesoporous silica shell guarantees good dispersibility of the Au@GMSN. Compared with single-component nanomaterials, the hybrid nanocomposite (i.e., graphene-coated cobalt nanoparticles,[24] graphene oxide/multi-walled carbon nanotube double layer,[32] and gold/graphene oxide nanohybrid films[33]) could lead to the synergistic effect in the enhancement of the LDI efficiency of analytes. It has been demonstrated that the gold nanoparticles could present the unique properties of high optical adsorption efficiency, low heat capacity, and high thermal conductivity,[34,35] which are propitious to the surface desorption/ionization process. Herein, the gold nanoparticles are embedded into the center part of the graphitized mesoporous silica shell, to endow the hybrid nanocomposite of Au@GMSN with the great synergistic effect for the laser desorption/ionization. To the best of our knowledge, no attempt has yet been made to synthesize the core−shell structured Au@GMSN and apply it as the surface-assisted material for SALDI-TOF MS in the sensitive detection of small molecules. The synthetic protocol of the Au@GMSN and the procedure for the detection of small molecules with Au@GMSN as surface-assisted material in SALDI-TOF MS are illustrated in Scheme 1.

Scheme 1. (a) Schematic Diagram of Au@GMSN; (b) SALDI-TOF MS Analysis Using Au@GMSN as Surface-Assisted Material

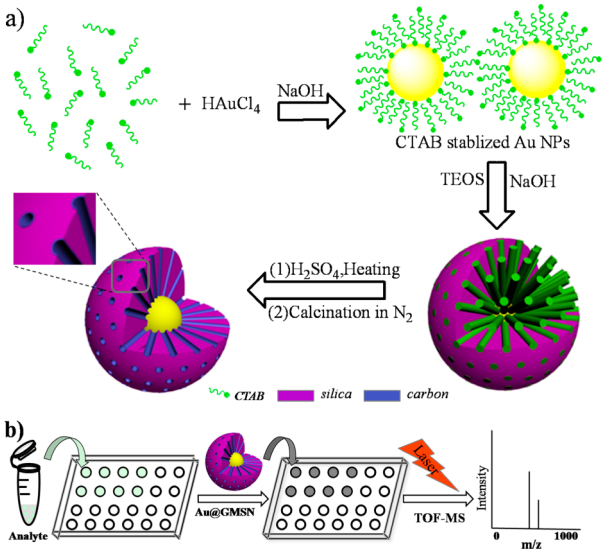

EXPERIMENTAL SECTION

Materials and Reagents. Tetrachloroaurate, rutin trihydrate, trisodium citrate, ammonium nitrate, and sodium hydroxide were purchased from Sinopharm Chemical Reagent Co., Ltd. (Shanghai, China). Cetyltrimethylammonium bromide (CTAB, 99.0 wt %), morin hydrate, 2,5-dihydroxybenzoic acid (DHB), and tetraethyl orthosilicate (TEOS, 98.0 wt %) were purchased from Sigma−Aldrich (St. Louis, MO). 6,7-Dihydroxycoumarin was purchased from Heowns (Tianjin, China). D-(+)-xylose, D-galactose, D(+)-raffinose pentahydrate, D-(+)-trehalose dihydrate, puerarin, L-tryptophan, L-histidine, D,L-arginine, L-phenylalanine, berberine hydrochloride and curcumin were purchased from Aladdin (Shanghai, China). Tripeptide (L-γ-glutamyl-L-cysteinylglycine, glutathione/GSH), and dipeptide (phenylalanine-glutamic acid, F-E) were purchased from China Peptides (Shanghai, China). Sulfuric acid (H_2SO_4), hydrochloric acid (HCl), and ethanol were of analytical grade. Deionized water was purified with a Milli-Q water system (Millipore, USA).

Synthesis of Gold@Graphitized Mesoporous Silica Nanocomposite (Au@GMSN) And Gold@Mesoporous Silica Nanocomposite (Au@MSN). First, gold@mesoporous silica/CTAB nanocomposite was synthesized according to the literature, with slight modification.[36] A quantity of 0.640 g of CTAB was dissolved in a solution of 100 mL of water and 40 mL of ethanol, and the mixture was heated to 70 °C under vigorous mechanical stirring. Next, 55 mg of tetrachloroaurate was added and stirred at 70 °C for 5 min. Then, 0.2 mL of 2 M NaOH was added. After stirring for 30 min, the resulting aqueous solution was diluted with 100 mL of water. Then, 1 mL of tetraethyl orthosilicate and 0.8 mL of 2 M NaOH were added in sequence, with a 5 min interval. The resulting mixture was stirred for 2 h at 70 °C. The resulting nanoparticles were centrifugated, washed four times with water, and finally vacuum-dried overnight at 60 °C obtain the gold@mesoporous silica/CTAB nanocomposite. The as-prepared gold@mesoporous silica/CTAB nanocomposite was dispersed in 2% H_2SO_4 and stirred for 30 min. Then, the mixture was dried at 100 °C for 12 h and subsequently heated for 12 h at 160 °C. The resulting material was carbonization at 600 °C under a nitrogen flow for 3 h. In order to increase the activated Si−OH, the carbonization product was dispersed in 50 mL of HCl (0.1 M) and stirred at 50 °C for 3 h to obtain the gold@graphitized mesoporous silica nanocomposite, hereafter called Au@GMSN. For the synthesis of gold@mesoporous silica nanocomposite (Au@MSN), the as-prepared gold@mesoporous silica/CTAB nanocomposite was refluxed in a 1 M ammonium nitrate ethanol/water solution (volume ratio of 1:2) for 24 h. The products was washed with ethanol three times and then dried under vacuum at 60 °C overnight.

Synthesis of Gold Nanoparticles. The gold nanoparticles were synthesized according to published procedures.[37] A 50-mL aqueous solution containing 4 mM of trisodium citrate was heated to boil under reflux with stirring in a round-bottomed flask, and then 0.25 mL of 200 mM $HAuCl_4$ was rapidly added into the boiled solution. The mixture was heated under reflux for 3 min, during which time the solution changed color from pale yellow to purple and then to wine-red. The flask was set aside until the solution had cooled to room temperature.

Preparation of Graphitized Mesoporous Silica Nanoparticle (GMSN). Briefly, 150 mg of CTAB was dissolved in 120 mL of water, followed by the addition of 0.5 mL of 2 M NaOH. After mechanically stirred for 30 min at 70 °C, 1.25 mL TEOS was added and stirred at 70 °C for another 2 h. The products were thoroughly washed with ethanol and water for several times, and finally vacuum-dried to obtain mesoporous silica/CTAB nanocomposite. The subsequent treatment was similar to that of Au@GMSN.

Sample Preparation for MALDI- or SALDI-TOF MS. The stock solutions of amino acids (L-tryptophan, L-histidine, D,L-arginine and L-phenylalanine), saccharide (D-(+)-xylose, D-galactose, D-(+)-trehalose dihydrate, and D-(+)-raffinose pentahydrate), and peptides (GSH and F-E) were prepared by dissolving the chemicals separately in water at a concentration of 1 mM. Traditional Chinese medicine (6,7-dihydroxycoumarin, morin hydrate, puerarin, rutin trihydrate, berberine hydrochloride, and curcumin) were dissolved in water/acetonitrile (1:1, v/v) to obtain the 1 mM stock solutions. Sample solutions at other concentrations were obtained by step dilution. All solutions were kept at ~4 °C for further use.

The DHB matrix (10 mg) was dissolved in 1 mL of water/acetonitrile (1:1, v/v) containing 0.1% TFA. GMSN (10 mg), Au@MSN (10 mg) and Au@GMSN (10 mg) were dispersed separately in 1 mL of water/ethanol (1:1, v/v) and sonicated for 30 min each. A quantity of 0.5 μL of analyte solution was pipetted onto the stainless steel plate, followed by drying under ambient conditions. Then, 0.5 μL of the suspension (DHB, GMSN, AuNPs, Au@MSN, or Au@GMSN) was pipetted onto the layer of analyte and dried under ambient conditions prior to MALDI- or SALDI-TOF MS measurements.

DOI: 10.1021/am507894y
ACS Appl. Mater. Interfaces 2015, 7, 2032−2038

Pre-enrichment Using Au@GMSN as Adsorbent and Matrix for Analysis of Compounds Containing Aromatic Ring Structures by SALDI-TOF MS. Au@GMSN (10 mg) was suspended in water (1 mL) and sonicated for 30 min. Then, the suspension (80 μL) was pipetted immediately into 3 mL of analyte water solution, and the mixture was vortex-mixed for 30 min. After centrifugation at 12 000 rpm for 10 min, the supernatant was removed, and the sediment was resuspended in 80 μL of water/ethanol (1:1, v/v) and pipetted onto the stainless steel plate. The stainless steel plate was left at room temperature for evaporation of the solvent and for further analysis by SALDI-TOF MS.

Characterization. All mass spectrometric analyses were carried out by using a AB SCIEX TOF/TOF 5800 (AB SCIEX, Shanghai, China) equipped with a neodymium:yttrium aluminum garnet (Nd:YAG) laser (355 nm wavelength) in positive reflective modes. All spectra were obtained by averaging 1000 laser shots, unless otherwise indicated. The laser irradiation point was automatically changed every 40 laser pulses, using the raster scan mode. The microscopy image was obtained using a Model ECLIPSE E100 microscope (Nikon, Japan) with an external light source. Transmission electron microscopy (TEM) measurements were carried out on a Model JEM-2000 EX (JEOL, Japan) microscope operated at 120 kV. Dynamic light scattering (DLS) measurements were made on a Zetasizer Nano ZS (ZEN3600) instrument (Malvern, England). Ultraviolet-visible light (UV-vis) absorption spectra were measured on a double-beam UV-vis spectrophotometer (Model UV-8000S, Metash, Shanghai, China) at a wavelength of 190−1100 nm. Nitrogen sorption isotherms were measured at 77 K with a Model QuadraSorb SI4 (Quantachrome Instruments, USA) system. Prior to the measurement, samples were degassed at 150 °C for 12 h. Raman spectra were taken at room temperature on an inVia spectrometer (Renishaw, Hoffman Estates, IL) equipped with an argon-ion laser at an excitation wavelength of 514 nm.

RESULTS AND DISCUSSION

The gold@mesoporous silica/CTAB nanocomposite was first synthesized through the autoreduction of tetrachloroaurate ions in the presence of cetyltrimethylammonium bromide (CTAB), which acted as a template in the subsequent TEOS sol−gel polymerization process.[36] The pretreatment of gold@mesoporous silica/CTAB nanocomposite by 2% sulfuric acid was crucial for the successively conversion of CTAB to carbon, since CTAB was unstable at high temperature.[38,39] Then, the resulting solid particles were heated to 600 °C under a nitrogen flow to realize the formation of graphitized mesoporous silica shell. In the synthetic strategy being proposed here, CTAB polymers not only were employed as a template for creation of uniform mesopores, but also utilized as a carbon source for in situ generation of graphitized structure in the mesopores. The morphologies and structures of the prepared nanoparticles were characterized by transmission electron microscopy (TEM). As shown in Figure 1a, the Au@GMSN was quite uniform with spherical morphology, where each gold particle with diameter of ca. 10 nm was encompassed within an ordered mesoporous shell (ca. 30 nm in average thickness). The polydispersity index (PDI) obtained by dynamic light scattering (DLS) was 0.385, which indicated a relative monodispersity of Au@GMSN (see Figure S1 in the Supporting Information). The N_2 adsorption/desorption isotherms of Au@GMSN (Figure 1b) exhibit the type IV isotherm with a hysteresis loop, demonstrating the mesoporous characteristics. Au@GMSN has a high Brunauer−Emmett−Teller (BET) surface area of 800 m^2/g and a high pore volume of 0.998 cm^3/g. The density functional theory (DFT) pore size distribution curve confirms the uniform mesopore size of Au@GMSN centered around 3.5 nm (Figure 1b, inset). The elementary units of Au@GMSN−gold nanoparticles (Au NPs), graphitized mesoporous silica nanoparticle (GMSN), and gold@mesoporous silica nanocomposite (Au@MSN) were tested simultaneously (see Figure S2 in the Supporting Information). TEM images showed the successful preparation of Au NPs with a diameter of ca. 13 nm, (GMSN) with a diameter of ca. 60 nm and (Au@MSN) with a diameter of ca. 70 nm. At the excitation laser wavelength of 514 nm, the Raman spectra of GMSN and Au@GMSN (Figure 1c) consist of two characteristic bands, namely, the graphite-like band (G-band) at ~1600 cm^{-1} and the disorder-induced band (D-band) at ~1380 cm^{-1}. As has been well-documented, the G-band is related to the vibration of sp^2-hybridized C atoms,[40] which verified the presence of graphitic domains on GMSN and Au@GMSN. Since the hydrophobic graphitized carbon was decorated on the inner pore wall of the hydrophilic mesoporous silica by in situ graphitization of template polymers, the Au@GMSN can be well-dispersed in water or ethanol.

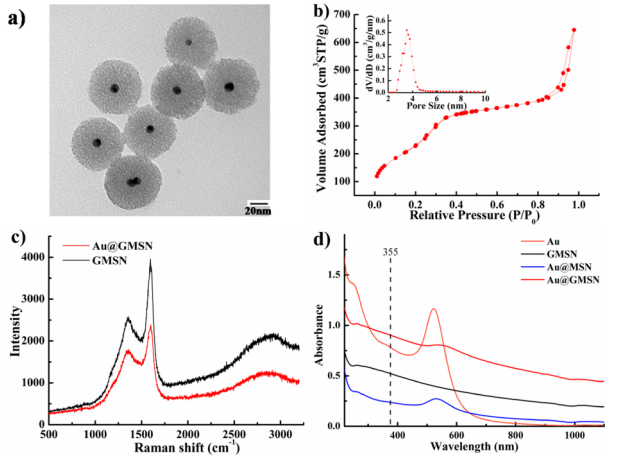

Figure 1. (a) TEM image of Au@GMSN; (b) nitrogen adsorption−desorption isotherms and pore size distribution (inset) of Au@GMSN; (c) Raman spectra (excitation at 514 nm) of the GMSN and Au@GMSN with the G and D bands of the graphitic carbon; and (d) UV-Vis spectra of Au, GMSN, Au@MSN, and Au@GMSN.

To perform SALDI-TOF MS analysis, the nanomaterials should be able to absorb photons from the pulsed laser. As shown in Figure 1d, Au@GMSN provided high absorption capability at 355 nm wavelength of the Nd:YAG laser, suggesting that Au@GMSN can meet the requirement to serve as a promising nanomaterial for SALDI-TOF MS. For comparison, the UV-vis absorption spectra of Au, GMSN, and Au@MSN were also measured at the same concentration. The order of UV absorption efficiency was Au@GMSN > Au > GMSN > Au@MSN. This trend foreshadows the synergistic effect of Au@GMSN on its SALDI-TOF MS application, since the LDI efficiency is linked to the optical properties of nanomaterials.[41] To further examine the laser desorption/ionization performance of the Au@GMSN in SALDI-TOF MS, amino acids (i.e., L-tryptophan, L-histidine, D,L-arginine and L-phenylalanine), saccharides (i.e., D-(+)-xylose, D-galactose, D-(+)-trehalose dihydrate, and D-(+)-raffinose pentahydrate) and tradition Chinese medicine (i.e., 6,7-dihydroxycoumarin, morin hydrate, puerarin, rutin trihydrate, berberine hydrochloride, and curcumin) were used as the test compounds. The chemical structures and molecular weights of these testing analytes are shown in Table S1 in the Supporting Information. Neutral saccharides remain a challenge to be detected by MALDI-TOF

DOI: 10.1021/am507894y
ACS Appl. Mater. Interfaces 2015, 7, 2032−2038

MS, because of the low ionization efficiency.[42,43] As shown in Scheme 1b, the SALDI-MS measurements were carried out by first pipetting analyte on the plate and then adding a suspension of Au@GMSN on the dried layer of analyte. All of the analytes were successfully detected with high sensitivity and clean mass spectra with low background noise peaks (see Figure 2). The dominant peaks for all of the analytes obtained from Au@GMSN were observed in their metal cation adduct forms of $[M+Na]^+$ and $[M+K]^+$, which could be ascribed to the residual alkali metal cations from the reagents used in the synthesis of Au@GMSN and/or in the preparation of analyte solutions.[32] To evaluate the sensitivity of SALDI-TOF MS with the assistance of Au@GMSN, the limits of detection (LOD) for all selected analytes were estimated. Each analyte was diluted with corresponding solvent at different ratios to obtain concentrations between 1 mM and 0.0001 mM. Figure S3 in the Supporting Information show the mass spectra of of amino acids, saccharides, and traditional Chinese medicine with a sample loading amount of 100 pmol. Along with the decrease in sample loading, the SALDI-TOF mass spectra still retain high resolution and low background interference. The LODs and the corresponding resolution for each analyte obtained in positive-ion mode are summarized in Table S2 in the Supporting Information. The lowest LOD of 50 fmol was observed in detection of berberine chloride. As demonstrated above, the Au@GMSN can be used to small-molecule analyses. Apart from the aforementioned analytes, SALDI-TOF-MS analysis of small peptides (e.g., L-γ-glutamyl-L-cysteinylglycine (GSH: m/z = 307) and phenylalanine-glutamic acid (F-E: m/z = 294)) has also been tested (see Figure S4 in the Supporting Information).

For the further comparison, the conventional organic matrix-DHB and the elementary units of Au@GMSN, Au NPs, GMSN and Au@MSN, were employed for LDI-TOF MS under the same conditions. Amino acids (i.e., L-phenylalanine, D,L-arginine, L-tryptophan, and L-histidine) were selected as the model analytes. The detailed TOF MS spectra are presented in Figure S5 in the Supporting Information). The organic matrix-DHB led to the abundant interfering matrix peaks in the low mass range (see Figure S5d). By contrast, there were no obvious interfering peaks for nanomaterials of Au@GMSN, Au, GMSN, and Au@MSN. The relative mass peak intensities obtained from Au@GMSN, Au@MSN, GMSN, and Au NPs are shown as bar graphs, for convenient comparison (Figure 3). The results showed that the ion intensities of amino acids desorbed from Au@GMSN were ~2 times higher than that from Au NPs and GMSN, indicating that the combination of Au NPs and GMSN was propitious to enhance the desorption/ionization efficiency of small analytes. The ion intensities of amino acids desorbed from Au@MSN were at least 20 times lower than that from Au@GMSN. The only difference between Au@GMSN and Au@MSN lied in the graphitized carbon deposited on the inner surface of the mesoporous silica shell. This demonstrated the importance of graphitized carbon in the enhancement of LDI efficiency. These results fully demonstrate that the as-synthesized Au@GMSN can induce synergistic effect and be a good alternative nanomaterial for SALDI-TOF MS.

Reproducibility is a commonly encountered problem in conventional MALDI-TOF MS. The signal reproducibility for berberine chloride was compared by using DHB and Au@GMSN as the matrixes. The relative standard deviations (RSDs) of signal intensities in three replicate analyses were 34%, 53% with DHB, and 5.5%, 8.0% with Au@GMSN for region-to-region and sample-to-sample assays, respectively. These results suggested that no "'sweet spot"' problem resulted from the use of Au@GMSN. Salt tolerance is another important factor for LDI-TOF MS in the analysis of biological

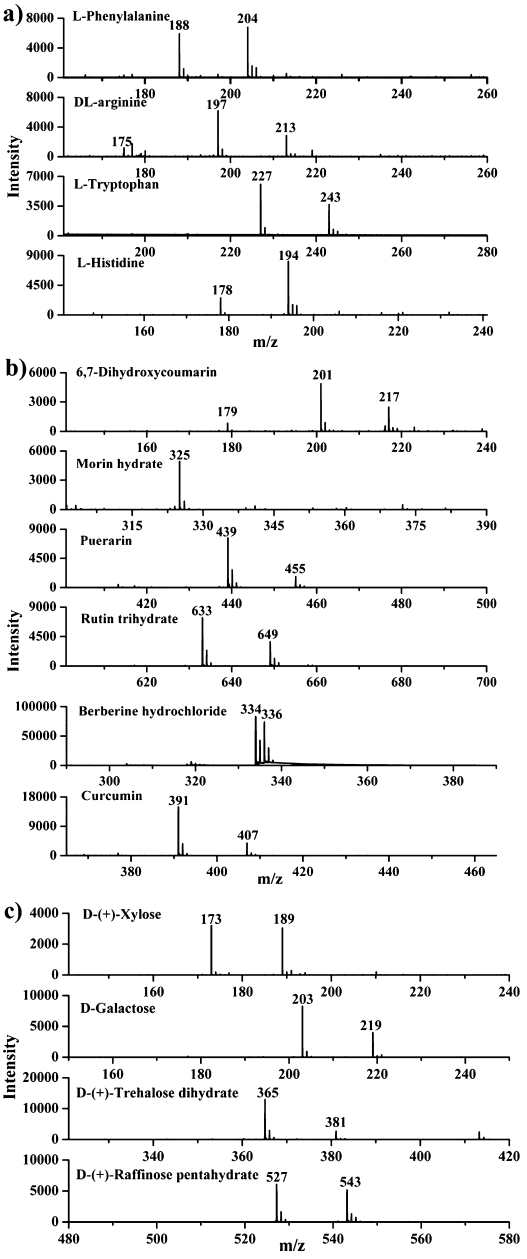

Figure 2. Mass spectra of (a) amino acids (L-phenylalanine: m/z = 188 $[M+Na]^+$ and 204 $[M+K]^+$; D,L-arginine: m/z = 197 $[M+Na]^+$ and 213 $[M+K]^+$; L-tryptophan: m/z = 227 $[M+Na]^+$ and 243 $[M+K]^+$; L-histidine: m/z = 178 $[M+Na]^+$ and 194 $[M+K]^+$); (b) traditional Chinese medicine (6,7-dihydroxycoumarin: m/z = 179 $[M+H]^+$, m/z = 201 $[M+Na]^+$ and 217 $[M+K]^+$; morin hydrate: m/z = 325 $[M+Na]^+$; puerarin: m/z = 439 $[M+Na]^+$ and 455 $[M+K]^+$; rutin trihydrate: m/z = 633 $[M+Na]^+$ and 649 $[M+K]^+$; berberine hydrochloride: m/z = 336 $[M-Cl]^+$; curcumin: m/z = 391 $[M+Na]^+$ and 407 $[M+K]^+$); and (c) saccharides (D-(+)-xylose: m/z = 173 $[M+Na]^+$ and 189 $[M+K]^+$; D-galactose: m/z = 203 $[M+Na]^+$ and 219 $[M+K]^+$; D-(+)-trehalose dihydrate: m/z = 365 $[M+Na]^+$ and 381 $[M+K]^+$); D-(+)-raffinose pentahydrate: m/z = 527 $[M+Na]^+$ and 543 $[M+K]^+$) with Au@GMSN as surface-assisted material for SALDI-TOF MS in positive-ion mode. The amount of each analyte is 500 pmol.

DOI: 10.1021/am507894y
ACS Appl. Mater. Interfaces 2015, 7, 2032−2038

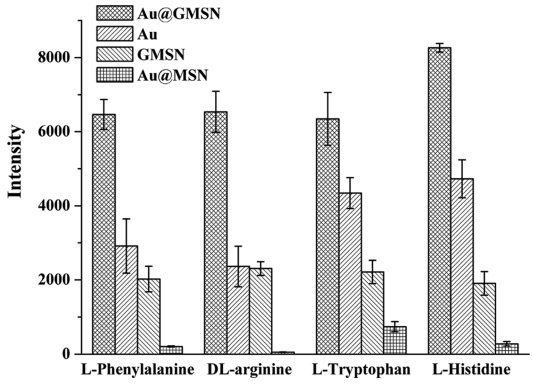

Figure 3. Comparison of mass peak intensities of various small molecules (including L-phenylalanine, D,L-arginine, L-tryptophan, and L-histidine) with four different nanoparticles as surface-assisted material for SALDI-TOF MS.

samples that usually contain a high concentration of salts. To evaluate the salt tolerance of Au@GMSN, mixtures of L-histidine, D,L-arginine, L-tryptophan, and L-phenylalanine with 0−1000 mM NaCl added were selected as the model analytes. For comparison, the traditional DHB was also employed as the matrix under the same conditions. As shown in Figure 4a, with

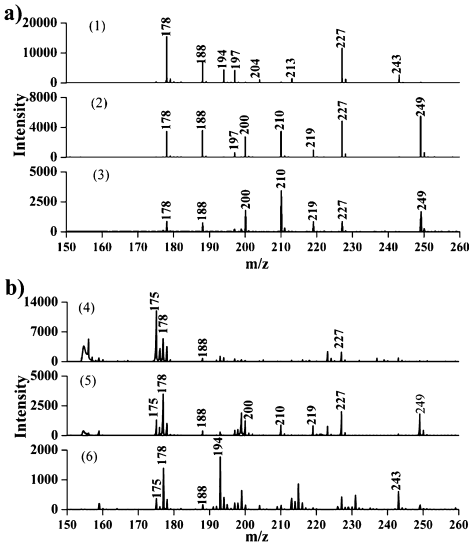

Figure 4. Mass spectra of samples containing L-histidine (m/z = 178 $[M+Na]^+$, m/z = 194 $[M+K]^+$, m/z = 200 $[M+2Na-H]^+$), D,L-arginine (m/z = 175 $[M+H]^+$, m/z = 197 $[M+Na]^+$, m/z = 213 $[M+K]^+$, m/z = 219 $[M+2Na-H]^+$), L-tryptophan (m/z = 227 $[M+Na]^+$, m/z = 243 $[M+K]^+$, m/z = 249 $[M+2Na-H]^+$), L-phenylalanine (m/z = 188 $[M+Na]^+$, m/z = 204 $[M+K]^+$, m/z = 210 $[M+2Na-H]^+$) obtained using (a) 10 mg/mL Au@GMSN and (b) 10 mg/mL DHB as matrixes. The amount of each analyte is 500 pmol. The samples were prepared in 0 mM NaCl (spectra 1 and 4), 500 mM NaCl (spectra 2 and 5), and 1000 mM NaCl (spectra 3 and 6).

Au@GMSN, the peaks for all of the amino acids were observed in potassium and/or sodium adduct ions (i.e., $[M+Na]^+$, $[M+K]^+$ or $[M+2Na-H]^+$). The acquired clean mass spectra have low background signals as well as high signal-to-noise (S/N) ratios and peak intensities, regardless of the amount of NaCl added. However, the proportion of doubly sodiated adducts to singly sodiated adducts was enhanced as the concentration of NaCl increased, which could be attributed to the excessive sodium salts providing sufficient ions for the analyte molecules in the ionization process. Figure 4b shows mass spectra of amino acids obtained from DHB, the strong background signals corresponding to the DHB-related ions strongly interfered with the peaks of amino acids, and there was a sharp decline in the signal intensities of amino acids as the concentration increase of NaCl. Clearly, the resolution and signal-to-noise obtained with DHB were far lower than that with Au@GMSN, no matter in the absence or presence of NaCl. The signal intensity obtained from DHB declined severely than that from Au@GMSN was because the high concentration of NaCl interfered with matrix crystal formation and caused signal suppression of the analytes.[44,45] However, for the Au@GMSN, it can form a homogeneous layer with the analytes and avoid complications with co-crystallization (as shown in Figure S6 in the Supporting Information). Based on the above observation, it can be concluded that the Au@GMSN has a higher salt tolerance than the organic matrix, which is very important for the direct analysis of samples without desalting in LDI-TOF MS.

To realize the sensitive detection of SALDI-TOF MS, the additional pre-enrichment ability of nanomaterial-based matrix is fascinating, since it can enhance the detection efficiency and avoid the complicated elution procedure during the conventional enrichment method prior to SALDI-TOF MS analysis.[46,47] In this manner, the nanomaterial first acts as an adsorbent and then serves as the matrix to transfer laser energy to the analytes for ionization, which requires not only the large capacity in enrichment but also great performance in UV energy absorption. Inspired from the large surface area of hydrophobic graphitized structures, as well as the above-confirmed UV energy absorption performance of the Au@GMSN, the sample enrichment-based laser desorption/ionization with the use of Au@GMSN was thus additionally carried out, with rutin trihydrate and curcumin chosen as the model molecules. (See Figure 5.) After enrichment, the signal

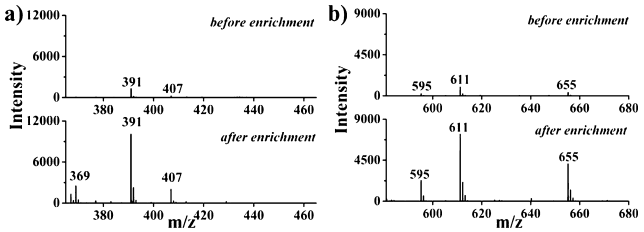

Figure 5. Mass spectra of (a) curcumin (m/z = 391 $[M+Na]^+$, m/z = 407 $[M+K]^+$) and (b) rutin trihydrate (m/z = 595 $[M+Na+H-K]^+$, m/z = 611 $[M+H]^+$, m/z = 655 $[M+2Na-H]^+$) analyzed by SALDI-TOF MS with Au@GMSN as the adsorbent and surface-assisted material.

intensities of the curcumin and rutin trihydrate with the concentration of 0.2 mM were increased 7.85- and 7.57-fold, respectively. Briefly, the results indicated that it was easy for Au@GMSN to capture compounds with aromatic ring structures, because of the hydrophobic and $\pi-\pi$ interaction between these compounds and Au@GMSN.

CONCLUSION

In summary, we have reported a novel core−shell-structured nanocomposite of Au@GMSN and explored its application on SALDI-TOF MS. The Au@GMSN integrates the large surface area of graphitic structure, highly ordered mesostructure, excellent dispersibility, and strong UV absorption into one

DOI: 10.1021/am507894y
ACS Appl. Mater. Interfaces 2015, 7, 2032−2038

nanosystem. With the assistance of Au@GMSN, small-molecular-weight compounds including amino acids, saccharides, peptides, and traditional Chinese medicine were sensitively detected in SALDI-TOF MS. The Au@GMSN demonstrated the advantages including low background interference, high LDI efficiency, good signal reproducibility, high salt tolerance. Moreover, the Au@GMSN could perform highly efficient enrichment of aromatic analytes for the on-surface sample preparation and detection of SALDI-TOF MS. Therefore, the Au@GMSN is a promising nanomaterial for SALDI-TOF MS in the sensitive and reproducible detection of small-molecular-weight compounds.

■ ASSOCIATED CONTENT

Ⓢ Supporting Information

Supporting figures and tables. This material is available free of charge via the Internet at http://pubs.acs.org.

■ AUTHOR INFORMATION

Corresponding Author

*E-mail: wurenan@dicp.ac.cn.

Notes

The authors declare no competing financial interest.

■ ACKNOWLEDGMENTS

The financial supports from the National Natural Science Foundation of China (Nos. 21175134 and 21375125) and the Creative Research Group Project of National Natural Science Foundation of China (No. 21321064) are greatly acknowledged.

■ REFERENCES

(1) Hillenkamp, F.; Karas, M.; Beavis, R. C.; Chait, B. T. Matrix-Assisted Laser Desorption/Ionization Mass Spectrometry of Biopolymers. *Anal. Chem.* **1991**, *63*, 1193A−1203A.

(2) Karas, M.; Hillenkamp, F. Laser Desorption Ionization of Proteins with Moleculars Masses Exceeding 10 000 Da. *Anal. Chem.* **1988**, *60*, 2299−2301.

(3) Zenobi, R.; Knochenmuss, R. Ion Formation in MALDI Mass Spectrometry. *Mass Spectrom. Rev.* **1998**, *17*, 337−366.

(4) Guo, Z.; Zhang, Q. C.; Zou, H. F.; Guo, B. C.; Ni, J. Y. A Method for the Analysis of Low-Mass Molecules by MALDI-TOF Mass Spectrometry. *Anal. Chem.* **2002**, *74*, 1637−1641.

(5) Tholey, A.; Heinzle, E. Ionic (Liquid) Matrices for Matrix-Assisted Laser Desorption/Ionization Mass Spectrometry—Applications and Perspectives. *Anal. Bioanal. Chem.* **2006**, *386*, 24−37.

(6) Tanaka, K.; Waki, H.; Ido, Y.; Akita, S.; Yoshida, Y.; Yoshida, T. Protein and Polymer Analyses up to *m/z* 100 000 by Laser Ionization Time-of-Flight Mass Spectrometry. *Rapid Commun. Mass Spectrom.* **1988**, *2*, 151−153.

(7) Wei, J.; Buriak, J. M.; Siuzdak, G. Desorption-Ionization Mass Spectrometry on Porous Silicon. *Nature* **1999**, *399*, 243−246.

(8) Go, E. P.; Apon, J. V.; Luo, G. H.; Saghatelian, A.; Daniels, R. H.; Sahi, V.; Dubrow, R.; Cravatt, B. F.; Vertes, A.; Siuzdak, G. Desorption/Ionization on Silicon Nanowires. *Anal. Chem.* **2005**, *77*, 1641−1646.

(9) Wang, C. M.; Reed, J. M.; Ma, L. Y.; Qiao, Y.; Luo, Y.; Zou, S. L.; Hickman, J. J.; Su, M. Biomimic Light Trapping Silicon Nanowire Arrays for Laser Desorption/Ionization of Peptides. *J. Phys. Chem. C* **2012**, *116*, 15415−15420.

(10) Seino, T.; Sato, H.; Yamamoto, A.; Nemoto, A.; Torimura, M.; Tao, H. Matrix-Free Laser Desorption/Ionization−Mass Spectrometry Using Self-Assembled Germanium Nanodots. *Anal. Chem.* **2007**, *79*, 4827−4832.

(11) Kawasaki, H.; Yao, T.; Suganuma, T.; Okumura, K.; Iwaki, Y.; Yonezawa, T.; Kikuchi, T.; Arakawa, R. Platinum Nanoflowers on Scratched Silicon by Galvanic Displacement for an Effective Saldi Substrate. *Chem.—Eur. J.* **2010**, *16*, 10832−10843.

(12) Xu, S. Y.; Li, Y. F.; Zou, H. F.; Qiu, J. S.; Guo, Z.; Guo, B. C. Carbon Nanotubes as Assisted Matrix for Laser Desorption/Ionization Time-of-Flight Mass Spectrometry. *Anal. Chem.* **2003**, *75*, 6191−6195.

(13) Hsu, W.-Y.; Lin, W.-D.; Hwu, W.-L.; Lai, C.-C.; Tsai, F.-J. Screening Assay of Very Long Chain Fatty Acids in Human Plasma with Multiwalled Carbon Nanotube-Based Surface-Assisted Laser Desorption/Ionization Mass Spectrometry. *Anal. Chem.* **2010**, *82*, 6814−6820.

(14) Shi, C. Y.; Deng, C. H.; Zhang, X. M.; Yang, P. Y. Synthesis of Highly Water-Dispersible Polydopamine-Modified Multiwalled Carbon Nanotubes for Matrix-Assisted Laser Desorption/Ionization Mass Spectrometry Analysis. *ACS Appl. Mater. Interfaces* **2013**, *5*, 7770−7776.

(15) Chen, S. M.; Zheng, H. Z.; Wang, J. N.; Hou, J.; He, Q.; Liu, H. H.; Xiong, C. Q.; Kong, X. L.; Nie, Z. X. Carbon Nanodots as a Matrix for the Analysis of Low-Molecular-Weight Molecules in Both Positive- and Negative-Ion Matrix-Assisted Laser Desorption/Ionization Time-of-Flight Mass Spectrometry and Quantification of Glucose and Uric Acid in Real Samples. *Anal. Chem.* **2013**, *85*, 6646−6652.

(16) Liu, C.-W.; Chien, M.-W.; Su, C.-Y.; Chen, H.-Y.; Li, L.-J.; Lai, C.-C. Analysis of Flavonoids by Graphene-Based Surface-Assisted Laser Desorption/Ionization Time-of-Flight Mass Spectrometry. *Analyst* **2012**, *137*, 5809−5816.

(17) Gulbakan, B.; Yasun, E.; Shukoor, M. I.; Zhu, Z.; You, M.; Tan, X.; Sanchez, H.; Powell, D. H.; Dai, H.; Tan, W. A Dual Platform for Selective Analyte Enrichment and Ionization in Mass Spectrometry Using Aptamer-Conjugated Graphene Oxide. *J. Am. Chem. Soc.* **2010**, *132*, 17408−17410.

(18) Dong, X. L.; Cheng, J. S.; Li, J. H.; Wang, Y. S. Graphene as a Novel Matrix for the Analysis of Small Molecules by MALDI-TOF MS. *Anal. Chem.* **2010**, *82*, 6208−6214.

(19) Zhang, J.; Dong, X. L.; Cheng, J. S.; Li, J. H.; Wang, Y. S. Efficient Analysis of Non-Polar Environmental Contaminants by MALDI-TOF MS with Graphene as Matrix. *J. Am. Soc. Mass Spectrom.* **2011**, *22*, 1294−1298.

(20) McLean, J. A.; Stumpo, K. A.; Russell, D. H. Size-Selected (2−10 nm) Gold Nanoparticles for Matrix Assisted Laser Desorption Ionization of Peptides. *J. Am. Chem. Soc.* **2005**, *127*, 5304−5305.

(21) Su, C.-L.; Tseng, W.-L. Gold Nanoparticles as Assisted Matrix for Determining Neutral Small Carbohydrates through Laser Desorption/Ionization Time-of-Flight Mass Spectrometry. *Anal. Chem.* **2007**, *79*, 1626−1633.

(22) Subra, G.; Mehdi, A.; Enjalbal, C.; Amblard, M.; Brunel, L.; Corriu, R.; Martinez, J. Functionalised Mesoporous Silica: A Good Opportunity for Controlled Peptide Oligomerisation. *J. Mater. Chem.* **2011**, *21*, 6321−6326.

(23) Tang, H. W.; Ng, K. M.; Lu, W.; Che, C. M. Ion Desorption Efficiency and Internal Energy Transfer in Carbon-Based Surface-Assisted Laser Desorption/Ionization Mass Spectrometry: Desorption Mechanism(s) and the Design of SALDI Substrates. *Anal. Chem.* **2009**, *81*, 4720−4729.

(24) Kawasaki, H.; Nakai, K.; Arakawa, R.; Athanassiou, E. K.; Grass, R. N.; Stark, W. J. Functionalized Graphene-Coated Cobalt Nanoparticles for Highly Efficient Surface-Assisted Laser Desorption/Ionization Mass Spectrometry Analysis. *Anal. Chem.* **2012**, *84*, 9268−9275.

(25) Shi, C. Y.; Meng, J. R.; Deng, C. H. Facile Synthesis of Magnetic Graphene and Carbon Nanotube Composites as a Novel Matrix and Adsorbent for Enrichment and Detection of Small Molecules by MALDI-TOF MS. *J. Mater. Chem.* **2012**, *22*, 20778−20785.

(26) Shi, C. Y.; Meng, J. R.; Deng, C. H. Enrichment and Detection of Small Molecules Using Magnetic Graphene as an Adsorbent and a Novel Matrix of MALDI-TOF-MS. *Chem. Commun.* **2012**, *48*, 2418−2420.

DOI: 10.1021/am507894y
ACS Appl. Mater. Interfaces 2015, 7, 2032−2038

(27) Hu, L. G.; Xu, S. Y.; Pan, C. S.; Yuan, C. G.; Zou, H. F.; Jiang, G. B. Matrix-Assisted Laser Desorption/Ionization Time-of-Flight Mass Spectrometry with a Matrix of Carbon Nanotubes for the Analysis of Low-Mass Compounds in Environmental Samples. *Environ. Sci. Technol.* **2005**, *39*, 8442−8447.
(28) Pan, C. S.; Xu, S. Y.; Hu, L. G.; Su, X. Y.; Ou, J. J.; Zou, H. F.; Guo, Z.; Zhang, Y.; Guo, B. C. Using Oxidized Carbon Nanotubes as Matrix for Analysis of Small Molecules by MALDI-TOF MS. *J. Am. Soc. Mass Spectrom.* **2005**, *16*, 883−892.
(29) Ma, R. N.; Lu, M. H.; Ding, L.; Ju, H. X.; Cai, Z. W. Surface-Assisted Laser Desorption/Ionization Mass Spectrometric Detection of Biomolecules by Using Functional Single-Walled Carbon Nanohorns as the Matrix. *Chem.—Eur. J.* **2013**, *19*, 102−108.
(30) Qin, H. Q.; Hu, Z. Y.; Wang, F. J.; Zhang, Y.; Zhao, L.; Xu, G. J.; Wu, R. A.; Zou, H. F. Facile Preparation of Ordered Mesoporous Silica−Carbon Composite Nanoparticles for Glycan Enrichment. *Chem. Commun.* **2013**, *49*, 5162−5164.
(31) Wang, Y.; Wang, K. Y.; Yan, X. Y.; Huang, R. Q. A General Strategy for Dual-Triggered Combined Tumor Therapy Based on Template Semi-Graphitized Mesoporous Silica Nanoparticles. *Adv. Healthcare Mater.* **2013**, *3*, 485−489.
(32) Kim, Y. K.; Na, H. K.; Kwack, S. J.; Ryoo, S. R.; Lee, Y.; Hong, S.; Hong, S.; Jeong, Y.; Min, D. H. Synergistic Effect of Graphene Oxide/MWCNT Films in Laser Desorption/Ionization Mass Spectrometry of Small Molecules and Tissue Imaging. *ACS Nano* **2011**, *5*, 4550−4561.
(33) Kim, Y. K.; Min, D. H. Preparation of the Hybrid Film of Poly(Allylamine Hydrochloride)-Functionalized Graphene Oxide and Gold Nanoparticle and Its Application for Laser-Induced Desorption/Ionization of Small Molecules. *Langmuir* **2012**, *28*, 4453−4458.
(34) Wang, G. R.; Wang, L. Y.; Qiang, R. D.; Wang, J. G.; Luo, J.; Zhong, C.-J. Correlation between Nanostructural Parameters and Conductivity Properties for Molecularly-Mediated Thin Film Assemblies of Gold Nanoparticles. *J. Mater. Chem.* **2007**, *17*, 457−462.
(35) Pełka, J. B.; Brust, M.; Gierłowski, P.; Paszkowicz, W.; Schell, N. Structure and Conductivity of Self-Assembled Films of Gold Nanoparticles. *Appl. Phys. Lett.* **2006**, *89*, 063110.
(36) Croissant, J.; Zink, J. I. Nanovalve-Controlled Cargo Release Activated by Plasmonic Heating. *J. Am. Chem. Soc.* **2012**, *134*, 7628−7631.
(37) Huang, M.-F.; Huang, C.-C.; Chang, H.-T. Improved Separation of Double-Stranded DNA Fragments by Capillary Electrophoresis Using Poly(Ethylene Oxide) Solution Containing Colloids. *Electrophoresis* **2003**, *24*, 2896−2902.
(38) Valle-Vigón, P.; Sevilla, M.; Fuertes, A. B. Mesostructured Silica−Carbon Composites Synthesized by Employing Surfactants as Carbon Source. *Microporous Mesoporous Mater.* **2010**, *134*, 165−174.
(39) Pang, J. B.; John, V. T.; Loy, D. A.; Yang, Z. Z.; Lu, Y. F. Hierarchical Mesoporous Carbon/Silica Nanocomposites from Phenyl-Bridged Organosilane. *Adv. Mater.* **2005**, *17*, 704−707.
(40) Datsyuk, V.; Kalyva, M.; Papagelis, K.; Parthenios, J.; Tasis, D.; Siokou, A.; Kallitsis, I.; Galiotis, C. Chemical Oxidation of Multiwalled Carbon Nanotubes. *Carbon* **2008**, *46*, 833−840.
(41) Guo, Z.; Ganawi, A. A. A.; Liu, Q.; He, L. Nanomaterials in Mass Spectrometry Ionization and Prospects for Biological Application. *Anal. Bioanal. Chem.* **2006**, *384*, 584−592.
(42) Harvey, D. J. Matrix-Assisted Laser Desorption/Ionization Mass Spectrometry of Carbohydrates. *Mass Spectrom. Rev.* **1999**, *18*, 349−450.
(43) Chang, Y.-L.; Liao, S. K.-S.; Chen, Y.-C.; Hung, W.-T.; Yu, H.-M.; Yang, W.-B.; Fang, J.-M.; Chen, C.-H.; Lee, Y. C. Tagging Saccharides for Signal Enhancement in Mass Spectrometric Analysis. *J. Mass Spectrom.* **2011**, *46*, 247−255.
(44) Garden, R. W.; Moroz, L. L.; Moroz, T. P.; Shippy, S. A.; Sweedler, J. V. Excess Salt Removal with Matrix Rinsing: Direct Peptide Profiling of Neurons from Marine Invertebrates Using Matrix-Assisted Laser Desorption Ionization Time-of-Flight Mass Spectrometry. *J. Mass Spectrom.* **1996**, *31*, 1126−1130.
(45) Monroe, E. B.; Koszczuk, B. A.; Losh, J. L.; Jurchen, J. C.; Sweedler, J. V. Measuring Salty Samples without Adducts with MALDI MS. *Int. J. Mass Spectrom.* **2007**, *260*, 237−242.
(46) Chen, W. Y.; Chen, Y. C. Affinity-Based Mass Spectrometry Using Magnetic Iron Oxide Particles as the Matrix and Concentrating Probes for SALDI MS Analysis of Peptides and Proteins. *Anal. Bioanal. Chem.* **2006**, *386*, 699−704.
(47) Kawasaki, H.; Akira, T.; Watanabe, T.; Nozaki, K.; Yonezawa, T.; Arakawa, R. Sulfonate Group-Modified FePtCu Nanoparticles as a Selective Probe for LDI-MS Analysis of Oligopeptides from a Peptide Mixture and Human Serum Proteins. *Anal. Bioanal. Chem.* **2009**, *395*, 1423−1431.

DOI: 10.1021/am507894y
ACS Appl. Mater. Interfaces 2015, 7, 2032−2038